

# Energy Efficient Power Allocation for Delay Constrained Cognitive Satellite Terrestrial Networks Under Interference Constraints

Yuhan Ruan<sup>1</sup>, *Member, IEEE*, Yongzhao Li<sup>2</sup>, *Senior Member, IEEE*, Cheng-Xiang Wang<sup>3</sup>, *Fellow, IEEE*,  
Rui Zhang<sup>4</sup>, *Member, IEEE*, and Hailin Zhang<sup>5</sup>, *Member, IEEE*

**Abstract**—With the ever increasing spectrum demand of broadband multimedia services, cognitive satellite terrestrial networks have emerged as a promising paradigm for future space information networks. To provide services with diverse delay quality-of-service (QoS) requirements in an energy-limited system, in this paper, we investigate energy efficient power allocation for cognitive satellite terrestrial networks. Employing statistical delay-QoS metric, power allocation schemes are formulated as optimization problems to maximize effective energy efficiency of secondary satellite communications while satisfying interference constraints imposed by primary terrestrial communications. Specifically, allowing for the availability of instantaneous channel state information (CSI) of the secondary transmitter-primary receiver link, optimal transmit powers are derived for both the cases of statistical and instantaneous interference constraints. Moreover, to provide a theoretical insight on the performance of the considered network, we derive closed-form expressions for the outage probability based on the obtained optimal transmit powers. The simulation results demonstrate the validity of the theoretical results and show the impacts of the delay exponent, interference constraint, and aggregate interference from terrestrial networks on the performance of satellite networks.

**Index Terms**—Cognitive satellite terrestrial networks, delay quality-of-service requirements, effective energy efficiency, interference constraints, outage performance.

Manuscript received August 30, 2018; revised April 3, 2019; accepted July 18, 2019. Date of publication August 2, 2019; date of current version October 9, 2019. This work was supported in part by the National Key Research and Development Program of China under Grant 254 and Grant 2018YFB1801101, in part by the National Natural Science Foundation of China under Grant 61771365, in part by the Natural Science Foundation of Shaanxi Province under Grant 2017JZ022, in part by the Postdoctoral Science Foundation of China under Grant 30101180044, in part by the 111 Project under Grant B08038, in part by the Fundamental Research Funds for the Central Universities under Grant JBF180101 and Grant 2242019R30001, and in part by EU H2020 RISE TESTBED Project under Grant 734325. The associate editor coordinating the review of this paper and approving it for publication was V. Cadambe. (*Corresponding author: Yongzhao Li.*)

Y. Ruan, Y. Li, R. Zhang, and H. Zhang are with the State Key Laboratory of Integrated Services Networks, Xidian University, Xi'an 710071, China (e-mail: ryh911228@163.com; yzhli@xidian.edu.cn; rui\_zhang\_xd@163.com; hlzhang@xidian.edu.cn).

C.-X. Wang is with the National Mobile Communications Research Laboratory, School of Information Science and Engineering, Southeast University, Nanjing 210096, China, and also with Purple Mountain Laboratories, Nanjing 211111, China (e-mail: chxwang@seu.edu.cn).

Color versions of one or more of the figures in this article are available online at <http://ieeexplore.ieee.org>.

Digital Object Identifier 10.1109/TWC.2019.2931321

## I. INTRODUCTION

**F**UTURE satellite communication systems are expected to provide high speed multimedia and broadband services. As a matter of fact, the satellite industry is targeting at not only areas without backbone connectivity (e.g., maritime, aeronautic, and other extreme remote sites), but also high dense populated scenarios with an existing communication infrastructure to decongest the terrestrial wireless network [1]. However, under exclusive regulation, currently deployed spectrum can hardly meet the ever increasing spectrum demand of resource-consuming multimedia applications in satellite communications [2], [3]. To accommodate more wireless services within the limited spectrum, cognitive radio has emerged as a promising technology to alleviate the scarcity of spectrum for satellite communications by enabling spectrum sharing between satellite and terrestrial networks, referred as cognitive satellite terrestrial networks [4], [5]. Various spectrum sharing approaches are suggested for cognitive satellite terrestrial networks, e.g., underlay, overlay, and interweave [6]. The underlay mode is especially attractive due to its high spectral efficiency, which allows cognitive systems to reuse the spectrum where incumbent signals are present without obstructing the normal operation of the primary licensed systems.

Although spectrum sharing in underlay mode can increase the system spectral efficiency, it would inevitably cause inter-system interference, which becomes a major challenge for cognitive satellite terrestrial networks and has drawn increasing attentions. Aiming at exploiting available spectrum, the authors in [7] proposed a joint interference-noise estimation algorithm to evaluate the interference between the terrestrial and satellite systems. Considering interference constraints imposed by primary terrestrial systems, performance analyses of multi-antenna cognitive satellite communications were conducted in [8] and [9] in terms of outage probability (OP) and ergodic capacity, respectively. Except for performance analysis, effective resource allocation, which is a key enabling technique to alleviate the mutual interference and ensure the coexistence of two networks, has also been widely studied. Particularly, the authors in [10] designed a cognitive zone to guarantee the primary satellite communication while providing high service availability to secondary terrestrial users. In [11], the authors conducted power allocation to maximize the achievable rate for cognitive hybrid satellite-terrestrial

networks with amplify-and-forward (AF) relays. The authors in [12] proposed a joint carrier-power-bandwidth allocation scheme to maximize the throughput of the satellite network, which operates in microwave frequency band. Besides, to enhance the physical layer security of cognitive satellite terrestrial networks, beamforming based secure transmissions were studied in [13] and [14].

The aforementioned studies mainly analyzed and optimized the performance degradation caused by interference, while ignoring the delay quality-of-service (QoS) requirements of end users. For future broadband satellite networks providing services with diverse QoS guarantees, e.g., in real-time or delay-sensitive applications, it is necessary to ensure that the delay adheres to service requirements [15], [16]. In this regard, effective capacity was introduced into satellite communications to characterize the system throughput with different delay-QoS requirements [17]. As illustrated in [17], extra transmit power is required to satisfy the delay-QoS constraints, especially when the constraint is relatively strict. Under this situation, power consumption is becoming a significant issue in cognitive satellite terrestrial networks with delay-QoS requirements. Moreover, since satellites are usually powered by energy-limited solar panels or batteries, efficient energy utilization<sup>1</sup> will prolong the lifetime of satellites and reduce the satellite mass, which is vital for the system design of future environment-friendly satellite terrestrial networks [20], [21]. Until now, energy efficient resource allocation schemes are mainly proposed for cognitive radio based terrestrial networks, e.g., [22] and [23]. For cognitive satellite terrestrial networks, only the authors in [24] conducted energy efficient power allocation in term of ergodic capacity and outage capacity, which cannot accurately evaluate the specific delay-QoS requirements of satellite terrestrial networks. To the best of our knowledge, energy efficient resource allocation for cognitive satellite terrestrial networks with various delay-QoS requirements has not been studied in the literature, which motivates the work of this paper. Taking both delay-QoS provisionings and energy efficiency (EE) requirements into account, effective energy efficiency metric which has been proposed in [25] and optimized in [26] for terrestrial wireless networks, provides a way for designing an elaborated power allocation scheme for cognitive satellite terrestrial networks in this paper.

On the other hand, in existing studies on cognitive satellite terrestrial networks, e.g., [8], [9], [11], [13], the instantaneous channel state information (CSI) of secondary transmitter-primary receiver (ST-PR) links was assumed perfectly known at the secondary transmitter. Although this assumption generally guarantees an instantaneous interference limitation at primary receivers (PRs), it is difficult to obtain such valuable CSI in practical communication systems, especially in cognitive satellite terrestrial networks where information exchange between satellite and terrestrial networks is limited [27].

<sup>1</sup>Both the static energy consumption (i.e., energy consumed to maintain the communication links active) and the dynamic energy consumption (i.e., energy consumed to transmit or receive traffics) have significant impacts on the energy efficiency of satellite systems [18]. In this paper, we focus on optimizing the transmit power to improve the energy efficiency, which is a common prospect for satellite communication systems [19].

For some scenarios, only statistical information of the ST-PR links is available at the secondary transmitter. Thus, considering the availability of the instantaneous CSI of ST-PR links, we propose two power allocation schemes for the considered network, where the interference constraints imposed by primary terrestrial network were guaranteed in a instantaneous and probabilistic manners, respectively. The contributions of this paper are summarized as follows:

- 1) Both delay-QoS provisionings and EE requirements are taken into account in the proposed power allocation schemes. Specifically, employing delay QoS exponent, we introduce a metric named as effective energy efficiency (eEE) into the cognitive satellite terrestrial network. Then, power allocation schemes are formulated as optimization problems to maximize eEE while satisfying interference constraints imposed by terrestrial communications.
- 2) Allowing for the availability of the instantaneous CSI of ST-PR links in practice, we consider two types of interference constraints in the power allocation, i.e., statistical and instantaneous interference constraints. Moreover, by converting the concave-convex eEE optimization problem to an equivalent convex problem with the Charnes-Cooper transformation, we derive the optimal solutions for the transmit power in both interference constraints cases.
- 3) Using the derived optimal transmit powers, we analyze the outage performance of cognitive satellite terrestrial networks, providing a theoretical insight on the system performance. In particular, to characterize a system-wide interference, we study a general scenario where the primary terrestrial transmitters are modeled as points of a Poisson point process (PPP). By analyzing the distribution of the aggregate interference, closed-form expressions for the OP are finally obtained.

The remainder of the paper is organized as follows. Section II introduces the system model. Section III analyzes the eEE and interference constraints associated with subsequent power allocation. Energy efficient power allocation schemes for the delay-constrained cognitive satellite terrestrial network under statistical and instantaneous interference constraints are investigated in Section IV and Section V, respectively. Simulation and numerical results are given in Section VI. Finally, conclusions are made in Section VII.

## II. SYSTEM MODEL

As shown in Fig. 1, we consider an underlay cognitive satellite terrestrial network, where the satellite (S) transmits signals to the destination (D) exploiting the spectrum bands allocated to the terrestrial cellular network. According to the coverage characteristics of satellite beams, there would be multiple primary transmitters (PTs) within the considered beam spot. In this case, the satellite will interfere the PRs while the destination will also suffer from the aggregate interference caused by  $N$  PTs. Considering the number and locations of PTs are random, we characterize the spatial distribution of PTs as a PPP with intensity  $\lambda$ . Without loss of generality,

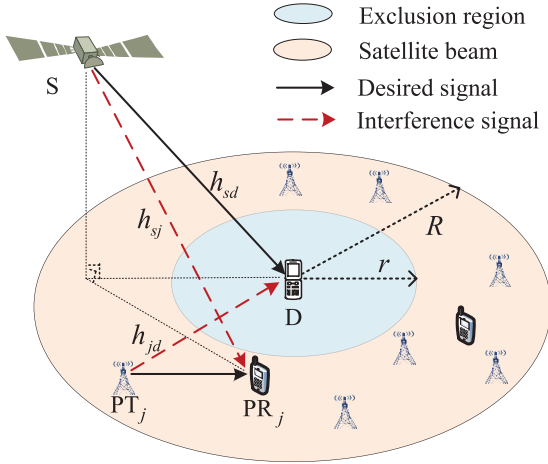


Fig. 1. System model of the underlay cognitive satellite terrestrial network.

$N$  PTs are assumed to be located in a finite annular area centered in the satellite receiver. The circle with radius  $r$  is the exclusion region, which plays an important role in protecting the sensitive satellite receiver from severe interference [28]. In addition,  $R$  denotes the outer radius, beyond which the interference from PTs is assumed to be negligible due to path loss. It is assumed that each node is equipped with a single antenna. We denote  $h_{sd}$ ,  $h_{sj}$ , and  $h_{jd}$  as the channel coefficients of  $S \rightarrow D$ ,  $S \rightarrow PR_j$ , and  $PT_j \rightarrow D$  links, respectively.

In this paper, satellite downlinks ( $h_{sd}, h_{sj}$ ) are modeled as independent shadowed-Rician fading channels, which are commonly used in evaluating wireless land mobile satellite (LMS) communication systems [29]. The probability distribution function (PDF) of  $|h_i|^2$  ( $i = sd, sj$ ), denoted by  $f_{|h_i|^2}(x)$ , is given as

$$f_{|h_i|^2}(x) = \alpha_i e^{-\beta_i x} {}_1F_1(m_i; 1; \delta_i x), \quad x > 0 \quad (1)$$

with

$$\begin{cases} \alpha_i = 0.5(2b_i m_i / (2b_i m_i + \Omega_i))^{m_i} / b_i \\ \beta_i = 0.5 / b_i \\ \delta_i = 0.5 \Omega_i / (2b_i^2 m_i + b_i \Omega_i). \end{cases}$$

Here,  $\Omega_i$  is the average power of line-of-sight component,  $2b_i$  is the average power of the multipath component,  $0 \leq m_i \leq \infty$  is the Nakagami parameter, and  ${}_1F_1(a; b; z)$  is the confluent hypergeometric function. For  $m_i = 0$ , the shadowed-Rician PDF reduces to Rayleigh PDF and for  $m_i = \infty$ , it converges to Rice PDF.

Meanwhile, we assume the power gain between  $PT_j$  and  $D$ ,  $|h_{jd}|^2$ , decays exponentially with parameter  $\alpha$  and follows Gamma distributions with a shape parameter  $k_{pd}$  and a scale parameter  $\eta_{pd}$ . As a result, the normalized aggregate interference from the PPP based PTs can be approximated as a gamma distribution with a shape parameter  $k_1 = \frac{(\mathbb{E}[I_a])^2}{\text{Var}[I_a]}$  and a scale parameter  $\eta_1 = \frac{\text{Var}[I_a]}{\mathbb{E}[I_a] N_0}$ , i.e.,  $I_a \sim \mathcal{G}(k_1, \eta_1)$  [30], where

$$\mathbb{E}[I_a] = 2\pi P_p \lambda \sqrt{\frac{k_{pd} + 1}{2k_{pd}}} \left( \frac{R^{2-\alpha} - r^{2-\alpha}}{2 - \alpha} \right) \quad (2)$$

and

$$\text{Var}[I_a] = \pi P_p^2 \lambda k_{pd} (1 + k_{pd}) \eta_{pd}^2 \left( \frac{R^{2-2\alpha} - r^{2-2\alpha}}{1 - \alpha} \right). \quad (3)$$

Thus, we have

$$f_{I_a}(x) = \frac{1}{\Gamma(k_1) \eta_1^{k_1}} x^{k_1-1} e^{-\frac{x}{\eta_1}} \quad (4)$$

where  $\Gamma(n) = \int_0^\infty x^{n-1} e^{-x} dx$  denotes the Gamma function, and  $\Gamma(n) = (n-1)!$  when  $n$  takes integer values [31, Eq. (8.310.1)].

### III. EFFECTIVE ENERGY EFFICIENCY AND INTERFERENCE CONSTRAINTS

Motivated by the demand for energy efficient design of cognitive satellite terrestrial networks with diverse services, this paper aims to implement power allocation to increase the EE while satisfying the delay-QoS requirements of satellite communications. In the following, we firstly analyze the effective capacity which incorporates the statistical delay-QoS into conventional channel capacity, followed by the definition of eEE. Afterwards, two kinds of interference constraints used in subsequent power allocation are introduced.

#### A. Effective Energy Efficiency

In the considered network, despite the time-varying nature of satellite channels, satellite service providers must guarantee a specified QoS to satisfy their customers who have various kinds of multimedia traffics. For this purpose, we make use of the concept of effective capacity, which is defined as the maximum constant arrival rate that a given service process can support under a given delay constraint, specified by the QoS exponent  $\theta$  [32]. Different from Shannon capacity without any restrictions on delay, the effective capacity ensures the maximum probabilistic delay for the incoming user traffic in the network. Specifically, for real-time traffic such as video conferencing, a stringent delay-bound needs to be guaranteed and the effective capacity turns to be the outage capacity. On the other hand, the non-real-time traffic such as data disseminations demands high throughput while a loose delay constraint is imposed, the effective capacity turns to be the ergodic capacity.

For a discrete-time, stationary, and ergodic stochastic service process  $\{R[t], t = 1, 2, \dots\}$ , the normalized effective capacity (in bits/s/Hz) is given by

$$\mathcal{C}(\theta) = -\frac{1}{\theta T_f B} \ln \left( \mathbb{E} \left\{ e^{-\theta T_f B R[t]} \right\} \right) \quad (5)$$

where  $\mathbb{E}\{\cdot\}$  denotes the expectation operator,  $B$  is the system bandwidth,  $T_f$  is the fading block length, and  $t$  is the time-index of the fading block. The QoS exponent  $\theta$  is a positive constant which represents the decaying rate of the QoS violation probability. Note that larger  $\theta$  corresponds to stricter QoS constraint, while smaller  $\theta$  implies looser QoS requirement. In the following discussions, the discrete time index  $t$  is omitted for simplicity. For the point-to-point satellite

link, the instantaneous service rate of one frame, denoted by  $R(\theta, v)$ , can be expressed as

$$R(\theta, v) = \log_2(1 + P_s(\theta, v)v) \quad (6)$$

where  $v = \frac{|h_{sd}|^2}{N_0(I_a+1)}$  is the channel-to-interference-plus-noise ratio,  $I_a = \sum_{j=1}^N \bar{\gamma}_p |h_{jd}|^2$  is the normalized aggregate interference received at the satellite receiver, and  $\bar{\gamma}_p = P_p/N_0$  with  $P_p$  as the transmit power of each PT and  $N_0$  as the average noise power. Taking the delay-QoS requirements into account, the transmit power of the satellite  $P_s$  is a function of  $\theta$  and  $v$ , i.e.,  $P_s(\theta, v)$ .

Considering both the statistical delay-QoS provisionings as well as EE requirement in cognitive satellite terrestrial networks, we aim to maximize the effective data-rate per unit energy. Toward this end, we define the eEE (in bits/Hz/Joule), denoted by  $\varsigma(\theta)$ , as the ratio of the achieved effective capacity (in bits/s/Hz) to the average power consumption (in Watt). Similar to the viewpoint of effective capacity, the effective energy efficiency means the achievable energy efficiency while satisfying a target delay requirement. Thus,  $\varsigma(\theta)$  of the cognitive satellite terrestrial network can be expressed as

$$\varsigma(\theta) = \frac{-\frac{1}{\theta T_f B} \ln(\mathbb{E}_v[e^{-\theta T_f B R(\theta, v)}])}{\mathbb{E}_v[P(\theta, v)]} \quad (7)$$

where  $P(\theta, v) = \eta P_s(\theta, v) + P_0^C + P_0^S$  denotes the total power consumption of the satellite, which consists of radio-frequency power  $\eta P_s(\theta, v)$ , circuit power  $P_0^C$ , and static power  $P_0^S$  with  $1/\eta \in (0, 1]$  denoting the drain efficiency of the power amplifier [33], [34]. Since the circuit and static power consumption are usually independent of data rate and regarded as a constant for the satellite, for notation simplicity, we use  $P(\theta, v) = \eta P_s(\theta, v) + P_0$  in the following, where  $P_0 = P_0^C + P_0^S$ . Thus,  $\varsigma(\theta)$  can be rewritten as

$$\varsigma(\theta) = \frac{-\frac{1}{\theta T_f B} \ln(\mathbb{E}_v[(1 + P_s(\theta, v)v)^{-\alpha}] )}{\mathbb{E}_v[\eta P_s(\theta, v)] + P_0} \quad (8)$$

where  $\alpha = \frac{\theta T_f B}{\ln(2)}$  is the normalized delay-QoS exponent.

### B. Interference Constraints

In cognitive satellite terrestrial networks, to reutilize the frequency band where primary terrestrial communication is operating, the secondary satellite communication should guarantee the interference power imposed to the PR below a predefined threshold  $I_{th}$ . The CSI of ST-PR links plays a critical role in protecting primary terrestrial communications as well as attaining spectrum access opportunities for secondary satellite communications. To restrict the instantaneous interference power received at the cellular user, the cellular user needs to feedback the real-time CSI of ST-PR links to the satellite, which means the perfect CSI is obtained at the expense of uplink bandwidth resources. Thus, the perfect CSI case is regarded as a relatively ideal case and provides an upper bound for the system performance. However, in practical instances, it is very challenging to obtain accurate CSI of ST-PR links due to feedback delay and dynamics of wireless

channels, especially in cognitive satellite terrestrial networks where the information exchange between the satellite and terrestrial networks is limited. Thus, according to the prior knowledge of the CSI of ST-PR links at the satellite, we study two types of interference constraints in this paper.

Firstly, when the satellite is only aware of the statistical CSI instead of the perfect instantaneous CSI, violating the peak interference-power constraint is inevitable. In this case, we can adopt the statistical interference constraint to satisfy the interference-power constraint in a probabilistic manner, i.e.,

$$\Pr\{P_s(\theta, v, h_{sp})|h_{sp}|^2 \leq I_{th}\} \geq \sigma \quad (9)$$

where  $\sigma$  is the interference probability threshold, representing the lower bound of the interference threshold maintaining probability. Here,  $h_{sp}$  is the channel coefficient between the satellite and the PR with the largest elevation angle among multiple PRs [35].

On the contrary, when instantaneous CSI of the ST-PR link is perfectly known at the satellite, it can be exploited to guarantee an instantaneous limitation of the interference at the terrestrial communications, i.e.,

$$P_s(\theta, v, h_{sp})|h_{sp}|^2 \leq I_{th}. \quad (10)$$

It is worth noting that both average and peak interference power constraints are generally employed to protect primary communications in a cognitive network. The difference of these two kinds of constraints falls into the fact that they are appropriate for different services from the perspective of protecting the PR's QoS [36]. This paper considers the peak interference power constraint as an example to investigate the power control problem in cognitive satellite terrestrial networks.

## IV. POWER ALLOCATION FOR DELAY-CONSTRAINED COGNITIVE SATELLITE TERRESTRIAL NETWORKS UNDER STATISTICAL INTERFERENCE CONSTRAINTS

In the following, we present energy efficient power allocation schemes for delay-constrained cognitive satellite terrestrial networks. Firstly, the statistical interference constraint in (9) is considered in this section. Specifically, we formulate the energy efficient power allocation as an optimization problem maximizing eEE subject to statistical interference limitations imposed by terrestrial communications. Since eEE maximization is a fractional programming problem and the statistical interference constraint is non-linear, the optimization problem is non-convex. To obtain the optimal transmit power, we convert the fractional programming problem to a convex problem with Charnes-Cooper transformations and replace the statistical interference constraint with its equivalent peak transmit power constraint. In addition, based on the obtained optimal solution of transmit power, we also analyze the outage performance to theoretically evaluate the impact of the delay and interference constraints on the performance of cognitive satellite terrestrial networks.

### A. Optimal Transmit Power Analysis

From (8) and (9), the energy efficient power allocation problem can be formulated as

$$\begin{aligned} & \underset{P_s(\theta, v, h_{\text{sp}}) \geq 0}{\text{maximize}} && \frac{-\frac{1}{\theta T_f B} \ln \left( \mathbb{E}_{v, h_{\text{sp}}} \left[ (1 + P_s(\theta, v, h_{\text{sp}}) v)^{-\alpha} \right] \right)}{\mathbb{E}_{v, h_{\text{sp}}} [\eta P_s(\theta, v, h_{\text{sp}})] + P_0} \\ & \text{subject to} && \Pr \left\{ P_s(\theta, v, h_{\text{sp}}) |h_{\text{sp}}|^2 \leq I_{\text{th}} \right\} \geq \sigma. \end{aligned} \quad (11)$$

As observed, the objective function in (11) is a ratio of two functions with respect to  $P_s(\theta, v, h_{\text{sp}})$ . As a result, the maximization of eEE is different from the effective capacity maximization problem, which is a monotone increasing function. Moreover, the interference constraint in a probability form can be rewritten as

$$\int_0^{\frac{I_{\text{th}}}{P_s(\theta, v)}} f_{|h_{\text{sp}}|^2}(x) dx \geq \sigma. \quad (12)$$

After integration, we can extract  $P_s(\theta, v)$  from (12) as

$$P_s(\theta, v) \leq P_M(\sigma) \quad (13)$$

where  $P_M(\sigma) = \frac{I_{\text{th}}}{F_{|h_{\text{sp}}|^2}^{-1}(\sigma)}$ ,  $F_{|h_{\text{sp}}|^2}^{-1}$  is the inverse cumulative distribution function of  $|h_{\text{sp}}|^2$ . For simplicity, we suppose that the Nakagami parameter  $m_i$  in the shadowed-Rician fading channel shown in (1) takes on integer values, i.e.,  $m_i \in \mathbb{N}$  [37]. Under this situation, we adopt the identity

$${}_1F_1(m_i; 1; \delta_i x) = e^{\delta_i x} \sum_{l=0}^{m_i-1} \frac{(-1)^l (1-m_i)_l (\delta_i x)^l}{(l!)^2} \quad (14)$$

where  $(u)_v = \Gamma(u+v)/\Gamma(u)$  is the Pochhammer symbol. Then,  $F_{|h_{\text{sp}}|^2}(x)$  can be expressed as

$$F_{|h_{\text{sp}}|^2}(x) = \alpha_{\text{sp}} \sum_{l=0}^{m_{\text{sp}}-1} \frac{(-1)^l (1-m_{\text{sp}})_l}{(l!)^2 (\beta_{\text{sp}} - \delta_{\text{sp}})^{l+1}} \Upsilon(l+1, (\beta_{\text{sp}} - \delta_{\text{sp}}) x) \quad (15)$$

where  $\Upsilon(\cdot, \cdot)$  denotes the lower incomplete Gamma function [31, Eq. (8.350.1)]. In this way, the statistical interference constraint is converted into a peak transmit power constraint.

In the following, we firstly provide a solution for the optimization problem without the transmit power constraint, i.e.,

$$\underset{P_s(\theta, v) \geq 0}{\text{maximize}} \frac{f(P_s(\theta, v))}{g(P_s(\theta, v))} = \frac{-\frac{1}{\theta T_f B} \ln \left( \mathbb{E}_v \left[ (1 + P_s(\theta, v) v)^{-\alpha} \right] \right)}{\mathbb{E}_v [\eta P_s(\theta, v)] + P_0}. \quad (16)$$

According to the Charnes-Cooper transformation [38], we apply suitable variable transformations to reformulate the optimization problem to an equivalent problem. By applying the transformations  $x = \frac{P_s(\theta, v)}{g(P_s(\theta, v))}$  and  $k = \frac{1}{g(P_s(\theta, v))}$ , we have

$$\begin{aligned} & \underset{P_s(\theta, v) \geq 0}{\text{maximize}} && k f \left( \frac{x}{k} \right) \\ & \text{subject to} && k g \left( \frac{x}{k} \right) = 1 \end{aligned} \quad (17)$$

where the equality constraint is not necessarily convex. Since  $P_s(\theta, v) v > 0$  and  $\alpha > 0$ ,  $(1 + P_s(\theta, v) v)^{-\alpha} < 1$  holds.

Thus, referring to the fact that  $-\frac{1}{\theta T_f B} < 0$  and  $\ln(x) < 0$  for  $0 < x < 1$ , we have  $f(P_s(\theta, v)) > 0$  for  $P_s(\theta, v) > 0$ . In the following, we use a relaxed problem according to Theorem 1 to obtain the closed-form expression of the optimal transmit power.

*Theorem 1:* Since  $f(P_s(\theta, v)) > 0$ , the problem in (17) is equivalent to the problem in (18).

$$\begin{aligned} & \underset{P_s(\theta, v) \geq 0}{\text{maximize}} && k f \left( \frac{x}{k} \right) \\ & \text{subject to} && k g \left( \frac{x}{k} \right) \leq 1. \end{aligned} \quad (18)$$

The proof is presented in Appendix A.

From Theorem 1, the optimization problem in (16) can be re-expressed as

$$\begin{aligned} & \underset{P_s(\theta, v) \geq 0}{\text{maximize}} && -\frac{1}{\theta T_f B} k \ln \left( \mathbb{E}_v \left[ (1 + P_s(\theta, v) v)^{-\alpha} \right] \right) \\ & \text{subject to} && k (\mathbb{E}_v [\eta P_s(\theta, v)] + P_0) \leq 1. \end{aligned} \quad (19)$$

The optimization problem in (19) can be converted to

$$\begin{aligned} & \underset{P_s(\theta, v) \geq 0}{\text{minimize}} && k \ln \left( \mathbb{E}_v \left[ (1 + P_s(\theta, v) v)^{-\alpha} \right] \right) \\ & \text{subject to} && k (\mathbb{E}_v [\eta P_s(\theta, v)] + P_0) \leq 1. \end{aligned} \quad (20)$$

By denoting  $f(P_s(\theta, v)) = \ln \left( \mathbb{E}_v \left[ (1 + P_s(\theta, v) v)^{-\alpha} \right] \right)$ , we can obtain that the second-order derivative of  $f(P_s(\theta, v))$  with respect to  $P_s(\theta, v)$  is positive. Thus,  $f(P_s(\theta, v))$  is convex in  $P_s(\theta, v)$ . Since the objective function in (20) is perspective of the function  $f$ , it is convex in  $P_s(\theta, v)$  [40]. Moreover, the constraint in (20) is a linear constraint. According to [41], the Karush-Kuhn-Tucker (KKT) conditions are both sufficient and necessary for the optimality of (20). Referring to  $P_s(\theta, v) = \frac{x}{k}$ , the Lagrangian associated with the problem in (20) can be given by

$$\begin{aligned} L(P_s(\theta, v), k, \lambda) &= k \ln \left( \mathbb{E}_v \left[ (1 + P_s(\theta, v) v)^{-\alpha} \right] \right) \\ &+ \lambda (k (\mathbb{E}_v [\eta P_s(\theta, v)] + P_0) - 1) \\ &= k \ln \left( \int (1 + P_s(\theta, v) v)^{-\alpha} f_v(v) dv \right) \\ &+ \lambda \left( k \left( \eta \int P_s(\theta, v) f_v(v) dv + P_0 \right) - 1 \right) \end{aligned} \quad (21)$$

where  $\lambda > 0$  is the Lagrangian parameter. Following similar procedures in [42], the first-order partial derivations of  $L(P_s(\theta, v), k, \lambda)$  on  $P_s(\theta, v)$ ,  $k$ , and  $\lambda$  can be written respectively as

$$k \frac{-\alpha v (1 + P_s(\theta, v) v)^{-\alpha-1} f_v(v)}{\mathbb{E}_v \left[ (1 + P_s(\theta, v) v)^{-\alpha} \right]} + \lambda k \eta f_v(v) = 0 \quad (22)$$

$$\ln \left( \mathbb{E}_v \left[ (1 + P_s(\theta, v) v)^{-\alpha} \right] \right) + \lambda (\mathbb{E}_v [\eta P_s(\theta, v)] + P_0) = 0 \quad (23)$$

$$k (\mathbb{E}_v [\eta P_s(\theta, v)] + P_0) = 1. \quad (24)$$

$$\begin{aligned}\mathbb{E}_v \left[ (1 + P'_s v)^{-\alpha} \right] &= \frac{\alpha_{\text{sd}} N_0}{\Gamma(k_1) \eta_1^{k_1}} \sum_{l=0}^{m_{\text{sd}}-1} \frac{(-1)^l (1 - m_{\text{sd}})_l (\delta_{\text{sd}} N_0)^l}{(l!)^2 \left( \frac{\alpha}{1+\alpha} + k_1 \right)} \frac{\tilde{k}_1! \alpha^{k_1}}{\tilde{\beta}_{\text{sd}}^{\tilde{k}_1+1} b^{k_1}} {}_2F_1 \left( \tilde{k}_1+1, \frac{\alpha}{1+\alpha} + k_1; \frac{\alpha}{1+\alpha} + k_1 + 1; -\frac{\alpha}{b \tilde{\beta}_{\text{sd}} \eta_1} \right) \quad (27) \\ \mathbb{E}_v [P'_s] &= \frac{\alpha_{\text{sd}} N_0}{\Gamma(k_1) \eta_1^{k_1}} \sum_{l=0}^{m_{\text{sd}}-1} \frac{(-1)^l (1 - m_{\text{sd}})_l (\delta_{\text{sd}} N_0)^l}{(l!)^2} \frac{\tilde{k}_1! \alpha^{k_1}}{\tilde{\beta}_{\text{sd}}^{\tilde{k}_1+1} b^{k_1}} \left[ \frac{1}{\left( \frac{\alpha}{1+\alpha} + k_1 \right)} \right. \\ &\quad \left. \times {}_2F_1 \left( \tilde{k}_1+1, \frac{\alpha}{1+\alpha} + k_1; \frac{\alpha}{1+\alpha} + k_1 + 1; -\frac{\alpha}{b \tilde{\beta}_{\text{sd}} \eta_1} \right) - \frac{1}{(1+k_1)} {}_2F_1 \left( \tilde{k}_1+1, k_1+1; k_1+2; -\frac{\alpha}{b \tilde{\beta}_{\text{sd}} \eta_1} \right) \right] \quad (28)\end{aligned}$$

Hence, from (22), the optimal transmit power can be written as

$$P'_s = \left[ \frac{\alpha^{\frac{1}{1+\alpha}}}{b^{\frac{1}{1+\alpha}} v^{\frac{\alpha}{1+\alpha}}} - \frac{1}{v} \right]^+ \quad (25)$$

where  $[x]^+ = \max(0, x)$  and  $b = \lambda \eta f_1(b)$ . Here,  $f_1(b) = \mathbb{E}_v \left[ (1 + P'_s v)^{-\alpha} \right]$  is the expectation which will be derived in the following. By inserting the transmit power in (25) into (23) and denoting  $f_2(b) = \mathbb{E}_v [P'_s]$ , we can get

$$f_1(b) \ln(f_1(b)) + b(P_0 + f_2(b)) = 0. \quad (26)$$

In (26), the involved mean values  $f_1(b)$  and  $f_2(b)$  can be derived as (27) and (28), shown at the top of this page.

The derivation steps can be found in Appendix B. After that, there is only one variable  $b$  in (26) and it can be obtained easily through the equality (26). Until now, we can clearly find that  $b$  involved in (25) is a constant only related to system parameters.

Assume that we have obtained the interference-unconstrained transmit power for maximizing eEE. When the interference constraint is considered, the optimization problem can be divided into two regions.

(1)  $P'_s \leq P_M(\sigma)$ : In this case, the transmit power maximizing eEE without interference constraints is lower than the transmit power restricted by the interference power of terrestrial communications. As such, the added interference constraint does not affect the optimal solution and hence, the optimal power of (11) is the same as that of (16), i.e.,  $P_s^* = P'_s$ .

(2)  $P'_s > P_M(\sigma)$ : If the required power for maximizing the unconstrained eEE beyond the interference level allowed by terrestrial communications, it would be invalid for practical system applications. Note that the optimization objective in (20) is a monotone decreasing function of transmit power. As a consequence, the optimal problem with interference constraint can be simplified into a transmit power constrained minimization problem, and we have  $P_s^* = P_M(\sigma)$ .

In summary, the optimal transmit power of (11) can be expressed as

$$P_s^* = \min \left( \left[ \frac{\alpha^{\frac{1}{1+\alpha}}}{b^{\frac{1}{1+\alpha}} v^{\frac{\alpha}{1+\alpha}}} - \frac{1}{v} \right]^+, P_M(\sigma) \right). \quad (29)$$

### B. Outage Analysis Based on the Optimal Transmit Power

We have obtained the optimal transmit power maximizing the eEE with interference constraints. To visualize the

effect of the power allocation scheme on the transmission performance, we investigate the performance of the secondary satellite system in terms of OP based on the derived solution in (29). The OP,  $\mathcal{P}_{\text{out}}$ , is defined as the probability that the instantaneous end-to-end signal-to-interference-plus-noise (SINR) falls below a threshold  $\Theta_{\text{th}}$ , i.e.,

$$\mathcal{P}_{\text{out}} = F_\gamma(\Theta_{\text{th}}) = \Pr(\gamma \leq \Theta_{\text{th}}) \quad (30)$$

where  $\gamma = P_s^* v$ . From (29), we can get

$$\gamma = \min \left( \left[ \left( \frac{\alpha v}{b} \right)^{\frac{1}{1+\alpha}} - 1 \right]^+, P_M(\sigma) v \right). \quad (31)$$

Since variables  $\alpha$ ,  $b$ , and  $P_M(\sigma)$  in (31) can be determined according to system parameters, the outage probability can be derived by integrating on  $v$ . As for any random variables  $a$  and  $b$ , we have  $\min(a, b) = a$  if  $b \geq a$  and  $\min(a, b) = b$  if  $b \leq a$ . Therefore, the OP can be expressed as the sum of following probabilities

$$\begin{aligned}\mathcal{P}_{\text{out}} &= \Pr \left( \left( \frac{\alpha v}{b} \right)^{\frac{1}{1+\alpha}} - 1 \leq P_M(\sigma) v, 0 \leq \left( \frac{\alpha v}{b} \right)^{\frac{1}{1+\alpha}} - 1 \leq \Theta_{\text{th}} \right) \\ &\quad + \Pr \left( \left( \frac{\alpha v}{b} \right)^{\frac{1}{1+\alpha}} - 1 \geq P_M(\sigma) v, P_M(\sigma) v \leq \Theta_{\text{th}} \right) \\ &= \underbrace{\Pr \left( P_M(\sigma) \geq \frac{\left( \frac{\alpha v}{b} \right)^{\frac{1}{1+\alpha}} - 1}{v}, \frac{b}{\alpha} \leq v \leq \frac{b \tilde{\Theta}_{\text{th}}^{1+\alpha}}{\alpha} \right)}_{\Psi_1} \\ &\quad + \underbrace{\Pr \left( P_M(\sigma) \leq \frac{\left( \frac{\alpha v}{b} \right)^{\frac{1}{1+\alpha}} - 1}{v}, P_M(\sigma) \leq \frac{\Theta_{\text{th}}}{v} \right)}_{\Psi_2} \quad (32)\end{aligned}$$

where  $\tilde{\Theta}_{\text{th}} = \Theta_{\text{th}} + 1$ . Note that  $\Psi_2$  can be divided into two parts as

$$\begin{aligned}\Psi_2 &= \underbrace{\Pr \left( \frac{b \tilde{\Theta}_{\text{th}}^{1+\alpha}}{\alpha} \leq v \leq \frac{\Theta_{\text{th}}}{P_M(\sigma)} \right)}_{\Psi_{21}} \\ &\quad + \underbrace{\Pr \left( P_M(\sigma) \leq \frac{\left( \frac{\alpha v}{b} \right)^{\frac{1}{1+\alpha}} - 1}{v}, \frac{b}{\alpha} \leq v \leq \frac{b \tilde{\Theta}_{\text{th}}^{1+\alpha}}{\alpha} \right)}_{\Psi_{22}}. \quad (33)\end{aligned}$$

Based on the observation that  $\Psi_1$  and  $\Psi_{22}$  can be combined, after some mathematical simplification, we can get

$$\mathcal{P}_{\text{out}} = \Pr\left(\frac{b}{\alpha} \leq v \leq \frac{\Theta_{\text{th}}}{P_M(\sigma)}\right) = \int_{\frac{b}{\alpha}}^{\frac{\Theta_{\text{th}}}{P_M(\sigma)}} f_v(x) dx. \quad (34)$$

To obtain  $\mathcal{P}_{\text{out}}$ , we firstly calculate the integrals on the intervals of  $[0, \frac{b}{\alpha}]$  and  $[\frac{b}{\alpha}, \frac{\Theta_{\text{th}}}{P_M(\sigma)}]$  with the aid of [31, Eq. (3.194.1)]. Then, the analytical expression of  $\mathcal{P}_{\text{out}}$  can be obtained as

$$\begin{aligned} \mathcal{P}_{\text{out}} &= \frac{\alpha_{\text{sd}} N_0}{\Gamma(k_1)} \sum_{l=0}^{m_{\text{sd}}-1} \frac{(-1)^l (1-m_{\text{sd}})_l (\delta_{\text{sd}} N_0)^l}{(l!)^2} \tilde{k}_1! \eta_1^{l+1} \\ &\times \left[ \left( \frac{\Theta_{\text{th}}}{P_M(\sigma)} \right)^{l+1} {}_2F_1\left(\tilde{k}_1+1, l+1; l+2; -\frac{\tilde{\beta}_{\text{sd}} \eta_1 \Theta_{\text{th}}}{P_M(\sigma)}\right) \right. \\ &\left. - \left( \frac{b}{\alpha} \right)^{l+1} {}_2F_1\left(\tilde{k}_1+1, l+1; l+2; -\frac{\tilde{\beta}_{\text{sd}} \eta_1 b}{\alpha}\right) \right]. \quad (35) \end{aligned}$$

## V. POWER ALLOCATION FOR DELAY-CONSTRAINED COGNITIVE SATELLITE TERRESTRIAL NETWORKS UNDER INSTANTANEOUS INTERFERENCE CONSTRAINTS

In previous section, we have derived the optimal transmit power for cognitive satellite terrestrial networks under statistical interference constraints. When the instantaneous CSI of the ST-PR link is available for the satellite, the instantaneous interference power constraint which sufficiently exploits the channel CSI makes much sense. Thus, in this section, we analyze the optimal transmit power under instantaneous interference constraints and the associated outage performance.

### A. Optimal Transmit Power Analysis

Under the instantaneous interference constraints as specified in (10), the power allocation problem can be formulated as

$$\begin{aligned} &\underset{P_s(\theta, v, h_{\text{sp}}) \geq 0}{\text{maximize}} \frac{-\frac{1}{\theta T_f B} \ln\left(\mathbb{E}_{v, h_{\text{sp}}}\left[(1+P_s(\theta, v, h_{\text{sp}})v)^{-\alpha}\right]\right)}{\mathbb{E}_{v, h_{\text{sp}}}\left[\eta P_s(\theta, v, h_{\text{sp}})\right] + P_0} \\ &\text{subject to } P_s(\theta, v, h_{\text{sp}}) |h_{\text{sp}}|^2 \leq I_{\text{th}}. \quad (36) \end{aligned}$$

For each specific transmission slot,  $h_{\text{sp}}$  remains unchanged and the interference received at the PR is determined by the transmit power. Thus, the interference constraint in (36) can be equalized to a transmit power constraint, i.e.,  $P_s(\theta, v) \leq P_m$ , where  $P_m = I_{\text{th}}/|h_{\text{sp}}|^2$ .

Similar to the analysis in subsection IV-A, the optimal transmit power under instantaneous interference constraints can be obtained as

$$P_s^* = \min\left(\left[\frac{\alpha^{\frac{1}{1+\alpha}}}{b^{\frac{1}{1+\alpha}} v^{\frac{\alpha}{1+\alpha}}} - \frac{1}{v}\right]^+, \frac{I_{\text{th}}}{|h_{\text{sp}}|^2}\right). \quad (37)$$

### B. Outage Analysis Based on the Optimal Transmit Power

From (37), the received SINR under instantaneous interference constraints can be written as

$$\gamma = \min\left(\left[\left(\frac{\alpha v}{b}\right)^{\frac{1}{1+\alpha}} - 1\right]^+, \frac{I_{\text{th}} v}{|h_{\text{sp}}|^2}\right). \quad (38)$$

Here, the outage probability should be derived by integrating on both  $v$  and  $|h_{\text{sp}}|^2$ . Similar to the derivation of (31), the OP under instantaneous interference constraints can be written as

$$\begin{aligned} \mathcal{P}_{\text{out}} &= \Pr\left(|h_{\text{sp}}|^2 \geq \frac{I_{\text{th}} v}{\Theta_{\text{th}}}, v \geq \frac{b \tilde{\Theta}_{\text{th}}^{1+\alpha}}{\alpha}\right) + \Pr\left(\frac{b}{\alpha} \leq v \leq \frac{b \tilde{\Theta}_{\text{th}}^{1+\alpha}}{\alpha}\right) \\ &\quad \underbrace{\hspace{10em}}_{\Psi_3} \quad \underbrace{\hspace{10em}}_{\Psi_4} \quad (39) \end{aligned}$$

where  $\Psi_3$  and  $\Psi_4$  can be calculated respectively as

$$\Psi_3 = \int_{\frac{b \tilde{\Theta}_{\text{th}}^{1+\alpha}}{\alpha}}^{\infty} \int_{\frac{I_{\text{th}} y}{\Theta_{\text{th}}}}^{\infty} f_{|h_{\text{sp}}|^2}(x) f_v(y) dx dy \quad (40)$$

and

$$\Psi_4 = \int_{\frac{b}{\alpha}}^{\frac{b \tilde{\Theta}_{\text{th}}^{1+\alpha}}{\alpha}} f_v(y) dy. \quad (41)$$

By defining  $\Psi_{31}$  as the inner integral of  $\Psi_3$ , and substituting (1) and (14) into the integral, we can get

$$\begin{aligned} \Psi_{31} &= \int_{\frac{I_{\text{th}} y}{\Theta_{\text{th}}}}^{\infty} f_{|h_{\text{sp}}|^2}(x) dx \\ &= \alpha_{\text{sp}} \sum_{q=0}^{m_{\text{sp}}-1} \frac{(-1)^q (1-m_{\text{sp}})_q \delta_{\text{sp}}^q}{(q!)^2} \int_{\frac{I_{\text{th}} y}{\Theta_{\text{th}}}}^{\infty} x^q e^{-\tilde{\beta}_{\text{sp}} x} dx \quad (42) \end{aligned}$$

where  $\tilde{\beta}_{\text{sp}} = \beta_{\text{sp}} - \delta_{\text{sp}}$ . According to [31, Eq. (3.381.3)], we can obtain

$$\Psi_{31} = \alpha_{\text{sp}} \sum_{q=0}^{m_{\text{sp}}-1} \frac{(-1)^q (1-m_{\text{sp}})_q \delta_{\text{sp}}^q}{(q!)^2 \tilde{\beta}_{\text{sp}}^{q+1}} \Gamma\left(q+1, \frac{\tilde{\beta}_{\text{sp}} I_{\text{th}} y}{\Theta_{\text{th}}}\right) \quad (43)$$

where  $\Gamma(n, x) = \int_x^{\infty} e^{-t} t^{n-1} dt$  denotes the upper incomplete Gamma function [31, Eq. (8.350.2)]. From [31, Eq. (8.352.2)], we have

$$\Gamma\left(q+1, \frac{\tilde{\beta}_{\text{sp}} I_{\text{th}} y}{\Theta_{\text{th}}}\right) = q! e^{-\frac{\tilde{\beta}_{\text{sp}} I_{\text{th}} y}{\Theta_{\text{th}}}} \sum_{s_1=0}^q \frac{\left(\frac{\tilde{\beta}_{\text{sp}} I_{\text{th}} y}{\Theta_{\text{th}}}\right)^{s_1}}{\Theta_{\text{th}}^{s_1} s_1!}. \quad (44)$$

By substituting (43), (44), and (55) into (40), and carrying out some mathematical manipulations,  $\Psi_3$  can be calculated as

$$\begin{aligned} \Psi_3 &= \frac{\alpha_{\text{sp}} \alpha_{\text{sd}} N_0}{\Gamma(k_1) \eta_1^{k_1}} \sum_{l=0}^{m_{\text{sd}}-1} \frac{(-1)^l (1-m_{\text{sd}})_l (\delta_{\text{sd}} N_0)^l}{(l!)^2} \tilde{k}_1! \\ &\times \sum_{q=0}^{m_{\text{sp}}-1} \frac{(-1)^q (1-m_{\text{sp}})_q \delta_{\text{sp}}^q}{q! \tilde{\beta}_{\text{sp}}^{q+1}} \sum_{s_1=0}^q \frac{\left(\tilde{\beta}_{\text{sp}} I_{\text{th}}\right)^{s_1}}{\Theta_{\text{th}}^{s_1} s_1!} \\ &\times \int_{\frac{b(1+\Theta_{\text{th}})^{1+\alpha}}{\alpha}}^{\infty} y^{s_1+l} e^{-\frac{\tilde{\beta}_{\text{sp}} I_{\text{th}} y}{\Theta_{\text{th}}}} \left(\frac{1}{\eta_1} + \tilde{\beta}_{\text{sd}} x\right)^{-\tilde{k}_1-1} dy. \quad (45) \end{aligned}$$

TABLE I  
LMS CHANNEL PARAMETERS [29]

$h_i$	Shadowing	$m_i$	$b_i$	$\Omega_i$
$h_{sp}$	Average shadowing (AS)	8	0.0129	0.372
$h_{sd}$	Infrequent light shadowing (ILS)	26	0.005	0.515
	Average shadowing (AS)	8	0.0129	0.372
	Frequent heavy shadowing (FHS)	2	0.0158	0.123

To derive this integral, we expand  $e^{-\frac{\tilde{\beta}_{sp} I_{th} y}{\Theta_{th}}}$  into series with  $L$  terms and then using [31, Eq. (3.194.2)], we can obtain  $\Psi_3$  as

$$\begin{aligned} \Psi_3 &= \frac{\alpha_{sp} \alpha_{sd} N_0}{\Gamma(k_1) \eta_1^{k_1}} \sum_{l=0}^{m_{sd}-1} \frac{(-1)^l (1-m_{sd})_l (\delta_{sd} N_0)^l}{(l!)^2} \tilde{k}_1! \\ &\times \sum_{q=0}^{m_{sp}-1} \frac{(1-m_{sp})_q \delta_{sp}^q}{q! \tilde{\beta}_{sp}^{q+1}} \sum_{s_1=0}^q \frac{1}{s_1!} \\ &\sum_{s_2=0}^L \frac{(-1)^{q+s_2} (\tilde{\beta}_{sp} I_{th})^{s_1+s_2}}{s_2! \Theta_{th}^{s_1+s_2}} \\ &\times \frac{\left(\frac{b}{\alpha}\right)^{s_1+s_2-k_1} (1+\Theta_{th})^{(1+\alpha)(s_1+s_2-k_1)}}{\tilde{\beta}_{sd}^{k_1+1} (k_1-s_1-s_2)} \\ &\times {}_2F_1\left(\tilde{k}_1+1, k_1-s_1-s_2; k_1-s_1-s_2+1; -\frac{\alpha}{\tilde{\beta}_{sd} \eta_1 b (\Theta_{th})^{1+\alpha}}\right). \end{aligned} \quad (46)$$

Similar to the derivation of (34), we can obtain the analytical expression of  $\Psi_4$  as

$$\begin{aligned} \Psi_4 &= \frac{\alpha_{sd} N_0}{\Gamma(k_1)} \sum_{l=0}^{m_{sd}-1} \frac{(-1)^l (1-m_{sd})_l (\delta_{sd} N_0)^l}{(l!)^2} \tilde{k}_1! \left(\frac{b \eta_1}{\alpha}\right)^{l+1} \\ &\times \left[ \tilde{\Theta}_{th}^{(1+\alpha)(l+1)} {}_2F_1\left(\tilde{k}_1+1, l+1; l+2; -\frac{\tilde{\beta}_{sd} \eta_1 b \Theta_{th}^{1+\alpha}}{\alpha}\right) \right. \\ &\left. - {}_2F_1\left(\tilde{k}_1+1, l+1; l+2; -\frac{\tilde{\beta}_{sd} \eta_1 b}{\alpha}\right) \right]. \end{aligned} \quad (47)$$

Finally, substituting (46) and (47) into (39), we can obtain the closed-form expression of the OP under instantaneous interference constraints.

## VI. RESULTS AND ANALYSIS

In this section, we evaluate the proposed power allocation schemes and conduct numerical simulations to corroborate our theoretical results. In the simulations, predetermined system parameters are given as follows. Specifically, we set the block length  $T_f = 2$  ms, system bandwidth  $B = 1$  MHz, the antenna gain at satellite  $G_t = 20$  dBi,  $\Theta_{th} = 0$  dB,  $\eta = 1.2$ ,  $N_0 = -114$  dBm, outer radius  $R = 10$  Km,  $PL_{sd} = PL_{sp} = 145$  dB,  $k_{pd} = 2$ , and  $\eta_{pd} = 0.5$ . The parameters of the shadowed-Rician LMS model are given in Table I, where the parameter  $m_i$  ( $i = sp, sd$ ) shows the intensity of fading and  $m_i$  increases as the amount of fading decreases. Unless specifically stated, the  $S \rightarrow PR$  and  $S \rightarrow D$  LMS

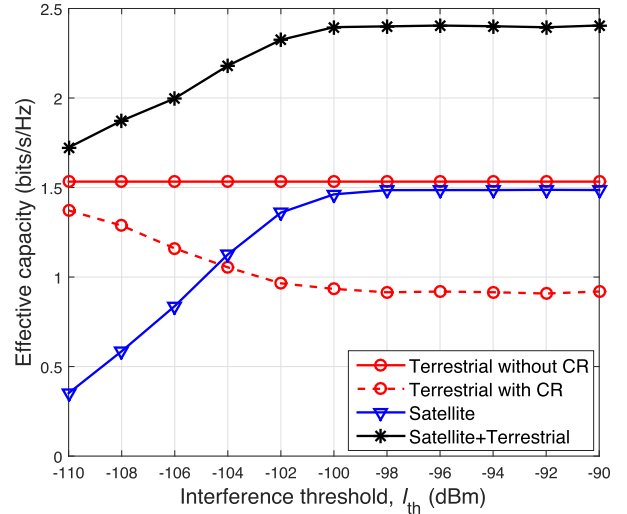


Fig. 2. System effective capacity comparison for the satellite terrestrial network with/without cognitive radio ( $\theta = 1 \times 10^{-3}$ ,  $P_p = 20$  dBm,  $r = 2$  Km,  $\lambda = 0.1$ ,  $\alpha = 3.8$ ,  $P_0 = 600$  mW).

channels are assumed to experience average shadowing (AS) in the simulations. In the following, by changing other system parameters, e.g., interference constraints  $I_{th}$ , interference probability threshold  $\sigma$ , delay QoS exponent  $\theta$ , transmit power of each PT  $P_p$ , inner radius  $r$ , PPP intensity  $\lambda$ , exponential parameter  $\alpha$ , and circuit power  $P_0$ , we obtain the numerical results of transmit power, effective energy efficiency, and outage probability.

To verify the benefits of incorporating cognitive radio into satellite terrestrial networks, we firstly compare the achievable effective capacity of the whole system with/without cognitive radio in Fig. 2. The terrestrial-only network before employing cognitive radio is regarded as a benchmark. In the considered underlay cognitive satellite terrestrial networks in this paper, spectrum sharing is allowed between the cognitive satellite system and the primary terrestrial network under reasonable interference management. In this way, satellite communication is enabled and corresponding capacity can be attained at the price of the capacity degradation of the terrestrial network. To protect the primary system from being obstructed, the interference power constraint is imposed on the transmit power of satellite communications. As observed, as the interference constraint gets looser, i.e.,  $I_{th}$  gets larger, the capacity of satellite (terrestrial) system increases (decreases) and remains a certain value eventually. Moreover, the total system capacity with cognitive radio is larger than that without cognitive radio. Specifically, we can achieve 14% system capacity gain when  $I_{th} = -110$  dBm and 57.9% gain when  $I_{th} = -100$  dBm.

Then, we conduct simulations to characterize the effects of different system parameters on the power allocation scheme of the satellite communication under statistical interference constraints. Fig. 3 plots the optimal transmit power according to the derived solution shown in (29) versus the interference probability threshold  $\sigma$  with various interfering configurations, illustrating the impact of the interference from primary terrestrial system on the secondary satellite system. From the

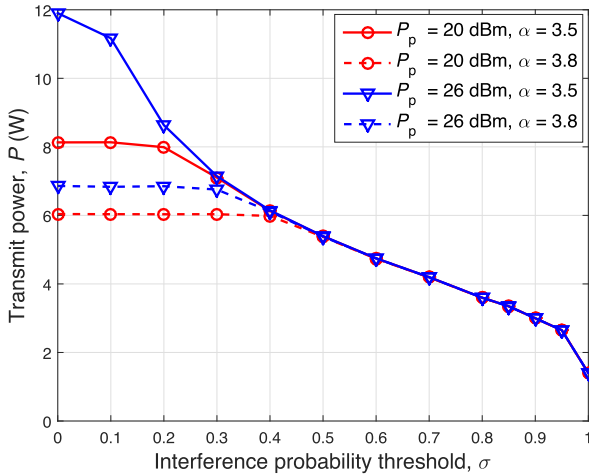


Fig. 3. The optimal transmit power versus interference probability threshold  $\sigma$  for various interfering configurations under statistical interference constraints ( $I_{th} = -95$  dBm,  $\theta = 5 \times 10^{-2}$ ,  $P_0 = 600$  mW,  $r = 1$  Km,  $\lambda = 0.5$ ).

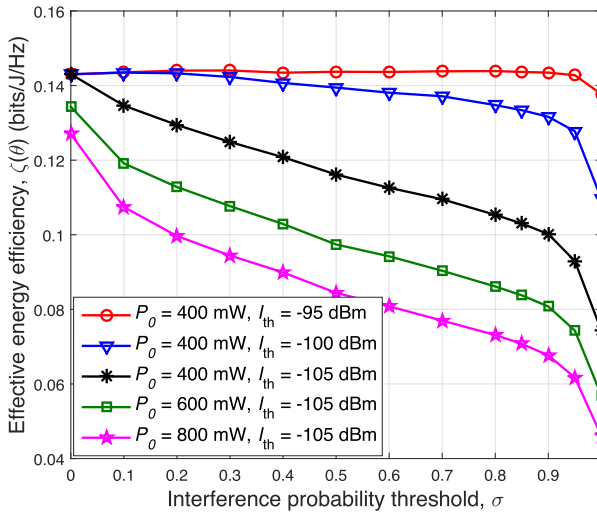


Fig. 4. Maximum achievable eEE versus interference probability threshold  $\sigma$  for various interference power constraints  $I_{th}$  and  $P_0$  under statistical interference constraints ( $\theta = 5 \times 10^{-2}$ ,  $P_p = 26$  dBm,  $\alpha = 3.8$ ,  $\lambda = 0.5$ ,  $r = 1$  Km).

figure we can see that the transmit power decreases as the interference probability threshold increases from 0 to 1, which determines the maximum allowable transmit power of the satellite. Moreover, the optimal transmit power increases when either the transmit power of PT ( $P_p$ ) increases or the quality of interference link increases (the link decays with a smaller exponent  $\alpha$ ), both of which determine the received interference power at the satellite receiver. This phenomenon indicates that when the communication link experiences a severer interference environment, the required transmit power is larger under a certain delay constraint. Furthermore, the curves with different interference parameters coincide with each other when  $\sigma$  falls in its relatively large region, illustrating that in this case the optimal transmit power is mainly restricted by the permitted maximum transmit power.

In Fig. 4, by substituting the optimal transmit power into the definition of eEE given in (7), we plot the achievable eEE of satellite communications versus the the interference

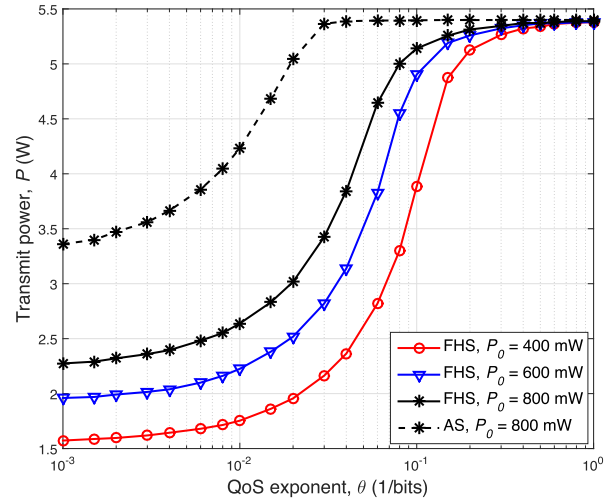


Fig. 5. The optimal transmit power versus the delay QoS exponent  $\theta$  for various fading cases and  $P_0$  under statistical interference constraints ( $I_{th} = -95$  dBm,  $\sigma = 0.5$ ,  $P_p = 26$  dBm,  $r = 1$  Km,  $\alpha = 3.8$ ,  $\lambda = 0.5$ ).

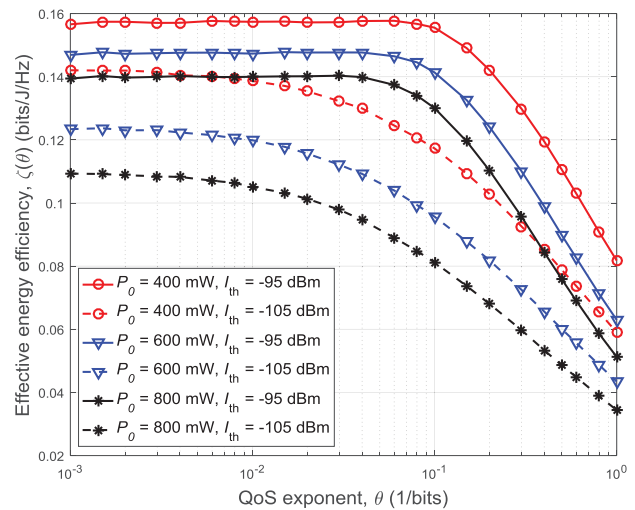


Fig. 6. Maximum achievable eEE versus delay exponent  $\theta$  for various interference power constraints  $I_{th}$  and  $P_0$  under statistical interference constraints ( $\sigma = 0.5$ ,  $P_p = 26$  dBm,  $r = 1$  Km,  $\lambda = 0.5$ ,  $\alpha = 4$ ).

probability threshold  $\sigma$  imposed by terrestrial communications. As observed, under a given interference power threshold  $I_{th}$ , the achievable eEE decreases as  $\sigma$  increases. In other words, for a given  $\sigma$ , the achievable eEE decreases with  $I_{th}$ . This phenomenon indicates that for the coexistence of satellite and terrestrial systems, there is a balance between the performance of two systems. Besides, larger  $P_0$  at the satellite results in a lower eEE of satellite communications.

Afterwards, we analyze the impact of the delay exponent  $\theta$  on the optimal transmit power and the achievable eEE in Fig. 5 and Fig. 6, respectively. Firstly, it can be seen from Fig. 5 that the optimal transmit power increases as  $\theta$  increases, which means as the delay constraint becomes stricter, more power is needed to satisfy the delay requirements, especially in a lighter fading case. Secondly, due to the existence of interference power constraints, the optimal transmit power of satellite systems becomes saturated eventually. Thirdly, the optimal transmit power increases as  $P_0$  increases, which implies

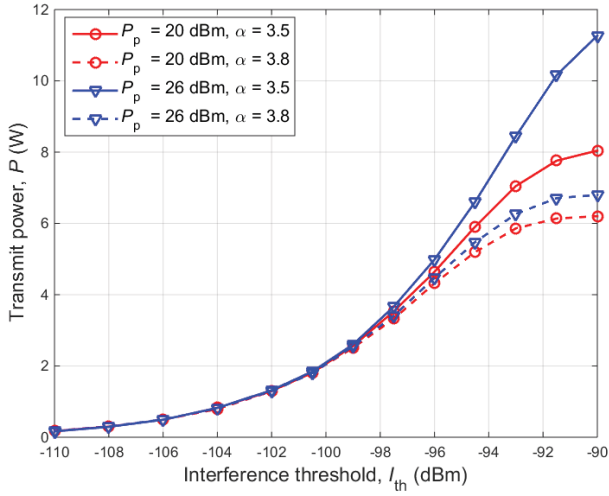


Fig. 7. The optimal transmit power versus the interference threshold  $I_{th}$  for various interfering configurations under instantaneous interference constraints ( $\theta = 5 \times 10^{-2}$ ,  $r = 1$  Km,  $\lambda = 0.5$ ,  $P_0 = 600$  mW).

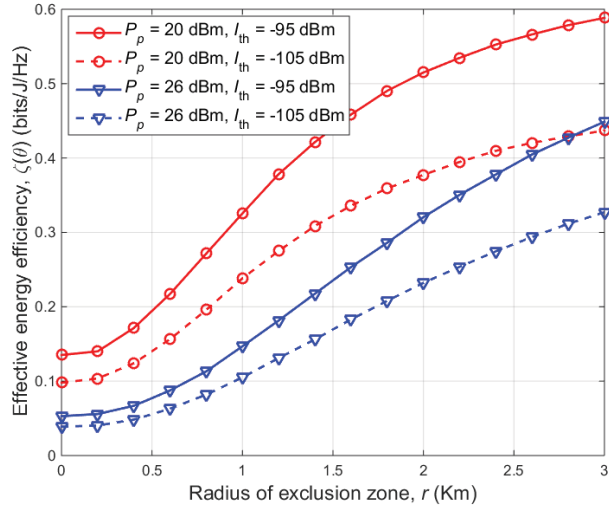


Fig. 8. Maximum achievable eEE versus the radius of exclusion region  $r$  for various interference power constraints  $I_{th}$  and  $P_p$  under instantaneous interference constraints ( $\theta = 5 \times 10^{-2}$ ,  $\lambda = 0.5$ ,  $\alpha = 3.8$ ,  $P_0 = 600$  mW).

that when circuit power consumption increases, we need to increase transmit power rather than decreasing it to achieve higher EE, although the total power consumption will increase. Moreover, Fig. 6 shows that the maximum achievable eEE decreases as the delay exponent increases or  $P_0$  increases. It is interesting to note that as  $P_0$  increases from 400 mW to 800 mW, the gap between the corresponding curves with different  $I_{th}$  increases, which implies that the effect of the interference constraints becomes more pronounced.

Next, we evaluate the performance of power allocation scheme under instantaneous interference constraints. Fig. 7 depicts the optimal transmit power according to the derived solution shown in (37) versus the interference threshold for various interfering configurations. As expected, the looser the interference power constraint is, i.e.,  $I_{th}$  gets larger, a higher optimal transmit power can be achieved.

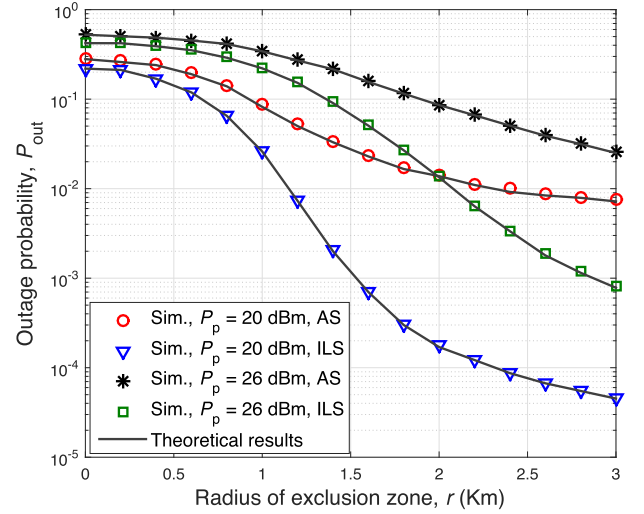


Fig. 9. OP versus the radius of exclusion region  $r$  for various transmit power of PT  $P_p$  and fading cases under statistical interference constraints ( $\sigma = 0.5$ ,  $I_{th} = -95$  dBm,  $\theta = 5 \times 10^{-2}$ ,  $\lambda = 0.5$ ,  $\alpha = 3.8$ ,  $P_0 = 600$  mW).

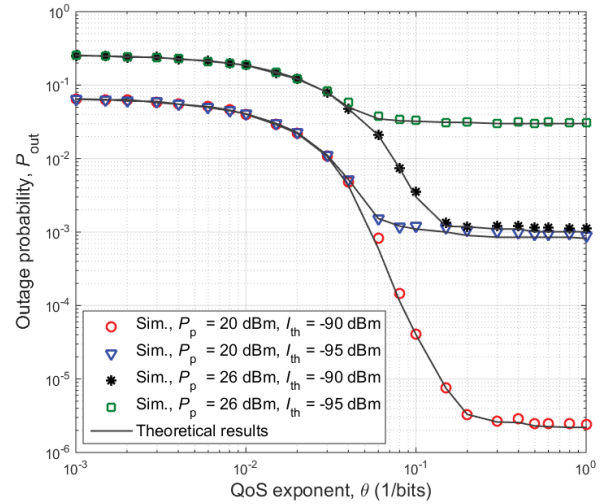


Fig. 10. OP versus delay exponent  $\theta$  for various interference power constraints  $I_{th}$  and transmit power of PT  $P_p$  with  $h_{sd}$  experiencing ILS fading under instantaneous interference constraints ( $r = 1$  Km,  $\lambda = 0.5$ ,  $\alpha = 3.8$ ,  $P_0 = 600$  mW).

Moreover, curves with different interfering configurations overlap when the interference threshold  $I_{th}$  is relatively small, since at this point, the optimal power is always obtained at its maximum power limited by interference threshold. Fig. 8 shows the achievable eEE versus the radius of exclusion zone  $r$ . We know that either the increment of  $P_p$  or the decrement of  $r$  will reduce the received SINR at the satellite receiver. In this case, more transmit power is required to satisfy the delay-QoS guarantees, which is similar to the observation in Fig. 3. Consequently, it would increase the total power consumption and result in a lower EE.

Finally, based on the obtained optimal transmit power, we evaluate the outage performance under statistical and instantaneous interference constraints in Fig. 9 and Fig. 10, respectively. Here, the simulation curves of outage probability are obtained by counting the numbers that the received SINR

is lower than the given threshold out of the total Monte Carlo trails, i.e.,  $10^8$ , and theoretical curves are plotted according to the derived expression of outage probability shown in (35) and (39), respectively. For both figures, we can observe that the theoretical results agree well with Monte Carlo simulations, confirming the accuracy of our derivations and simulations. As observed in Fig. 9, cases with light fading or small interference power from PTs can achieve a superior OP performance. Moreover, we can observe that when the satellite receiver is close to PTs, i.e.,  $r$  is small, the destination user will suffer from a particularly poor performance for the sever aggregate interference. Under this circumstances, a reasonable radius of the exclusion zone should be designed to guarantee the performance of both satellite and terrestrial networks. In Fig. 10, it can be seen that as the delay exponent  $\theta$  increases, the OP remains a constant at the beginning, then decreases and becomes saturated eventually. Moreover, the stricter the interference power constraint is, i.e.,  $I_{th}$  gets smaller, the larger the OP is, which also verifies the fact that there is a balance between the performance of two systems.

## VII. CONCLUSION

In this paper, we have investigated energy efficient power allocation for the delay-constrained cognitive satellite terrestrial network. Considering the requirements of energy efficient design for satellite terrestrial networks with statistical delay-QoS provisioning, we have investigated the power allocation scheme to maximize the eEE of satellite communications under the interference limitations imposed by terrestrial communications. Especially, both cases with statistical and instantaneous interference constraints have been considered. Based on the obtained optimal solutions of the transmit power, we have derived closed-form expressions of the OP to theoretically evaluate the system performance. Simulation results have demonstrated the validity of the theoretical results and shown that incorporating cognitive radio into satellite terrestrial network can enhance the system effective capacity. Moreover, the impacts of delay exponent and interference power threshold on the performance of the satellite network have been analyzed.

### APPENDIX A PROOF OF THEOREM 1

Here, we prove the theorem that since  $f(P_s(\theta, v)) > 0$ , the problem in (18) is equivalent to the problem in (17). Firstly, we denote  $\mathbb{P}_1$  and  $\mathbb{P}_2$  as the feasible set of (17) and (18). Then, we have

$$\mathbb{P}_1 = \left\{ x_1, k_1 \in \mathbb{R}_{++} \times \mathbb{R}_{++} : \frac{x_1}{k_1} \in \mathbb{P}, k_1 g\left(\frac{x_1}{k_1}\right) = 1 \right\} \quad (48)$$

$$\mathbb{P}_2 = \left\{ x_2, k_2 \in \mathbb{R}_{++} \times \mathbb{R}_{++} : \frac{x_2}{k_2} \in \mathbb{P}, k_2 g\left(\frac{x_2}{k_2}\right) \leq 1 \right\} \quad (49)$$

where  $\mathbb{R}_{++}$  is the set of positive real numbers. Obviously we have  $\mathbb{P}_1 \subseteq \mathbb{P}_2$ . To complete the proof, we should prove that all elements in  $\mathbb{P}_2 \setminus \mathbb{P}_1$  are suboptimal for (18). For any  $(x_2, k_2) \in \mathbb{P}_2$ , it holds that [39]

$$k_2 g\left(\frac{x_2}{k_2}\right) = \sigma \in (0, 1]. \quad (50)$$

Then, we assume that  $x_1 = x_2/\sigma$  and  $k_1 = k_2/\sigma$ , which indicate that for any  $(x_2, k_2) \in \mathbb{P}_2$ , there exists  $(x_1, k_1) \in \mathbb{P}_1$  and  $\sigma \in (0, 1]$ , so that  $(x_2, k_2) = (\sigma x_1, \sigma k_1)$ , where  $\sigma < 1$  if  $(x_2, k_2) \in \mathbb{P}_2 \setminus \mathbb{P}_1$ . Referring to the fact that the effective capacity function is non-negative, we can get

$$k_2 f\left(\frac{x_2}{k_2}\right) = \sigma k_1 f\left(\frac{x_1}{k_1}\right) \leq k_1 f\left(\frac{x_1}{k_1}\right). \quad (51)$$

Here, if  $(x_2, k_2) \in \mathbb{P}_2 \setminus \mathbb{P}_1$ , the inequality is strict. Until now, all the elements in  $\mathbb{P}_2 \setminus \mathbb{P}_1$  are suboptimal for the problem (18). This completes the proof of Theorem 1.

### APPENDIX B DERIVATION OF (27)

From the expression of  $P'_s$  specified in (25),  $\mathbb{E}_v \left[ (1 + P'_s v)^{-\alpha} \right]$  can be calculated as

$$\begin{aligned} \mathbb{E}_v \left[ (1 + P'_s v)^{-\alpha} \right] &= \mathbb{E}_v \left[ \left( \frac{\alpha v}{b} \right)^{-\frac{\alpha}{1+\alpha}} \right] \Bigg|_{v \geq \frac{b}{\alpha}} \\ &= \int_{\frac{b}{\alpha}}^{\infty} \left( \frac{\alpha x}{b} \right)^{-\frac{\alpha}{1+\alpha}} f_v(x) dx. \end{aligned} \quad (52)$$

To calculate the integral in (52), we need to derive the PDF of  $v$  firstly. From  $v = \frac{|h_{sd}|^2}{N_0(I_a+1)}$ ,  $f_v(x)$  can be written as

$$\begin{aligned} f_v(x) &= \int_0^{\infty} N_0(y+1) f_{I_a}(y) f_{|h_{sd}|^2}(N_0 x(y+1)) dy \\ &\stackrel{(a)}{=} \frac{\alpha_{sd} N_0}{\Gamma(k_1) \eta_1^{k_1}} \\ &\quad \times \int_0^{\infty} y^{k_1} e^{-\left(\frac{1}{\eta_1} + \beta_{sd} N_0 x\right)y} {}_1F_1(m_{sd}; 1; \delta_{sd} N_0 x y) dy. \end{aligned} \quad (53)$$

Here, (a) is obtained by approximating the interference dominates the noise, which is reasonable in an interference-limited scenario. By substituting (14) into (53) and carrying out some mathematical manipulation, we can obtain  $f_v(x)$  as

$$\begin{aligned} f_v(x) &= \frac{\alpha_{sd} N_0}{\Gamma(k_1) \eta_1^{k_1}} \sum_{l=0}^{m_{sd}-1} \frac{(-1)^l (1-m_{sd})_l (\delta_{sd} N_0)^l}{(l!)^2} x^l \\ &\quad \times \int_0^{\infty} y^{\tilde{k}_1} e^{-\left(\frac{1}{\eta_1} + \tilde{\beta}_{sd} x\right)y} dy \end{aligned} \quad (54)$$

where  $\tilde{k}_1 = k_1 + l$  and  $\tilde{\beta}_{sd} = (\beta_{sd} - \delta_{sd}) N_0$ . Using [31, Eq. (3.351.3)] we have

$$\begin{aligned} f_v(x) &= \frac{\alpha_{sd} N_0}{\Gamma(k_1) \eta_1^{k_1}} \sum_{l=0}^{m_{sd}-1} \frac{(-1)^l (1-m_{sd})_l (\delta_{sd} N_0)^l}{(l!)^2} \\ &\quad \times \tilde{k}_1! x^l \left( \frac{1}{\eta_1} + \tilde{\beta}_{sd} x \right)^{-\tilde{k}_1-1}. \end{aligned} \quad (55)$$

Then, substituting (55) into (52), we can get

$$\begin{aligned} \mathbb{E}_v \left[ (1 + P'_s v)^{-\alpha} \right] &= \frac{\alpha_{sd} N_0}{\Gamma(k_1) \eta_1^{k_1}} \sum_{l=0}^{m_{sd}-1} \frac{(-1)^l (1-m_{sd})_l (\delta_{sd} N_0)^l}{(l!)^2} \\ &\quad \times \tilde{k}_1! \left( \frac{\alpha}{b} \right)^{-\frac{\alpha}{1+\alpha}} \int_{\frac{b}{\alpha}}^{\infty} x^{l-\frac{\alpha}{1+\alpha}} \left( \frac{1}{\eta_1} + \tilde{\beta}_{sd} x \right)^{-\tilde{k}_1-1} dx. \end{aligned} \quad (56)$$

With the aid of [31, Eq. (3.194.2)], the analytical expression of  $\mathbb{E}_v \left[ (1 + P'_s v)^{-\alpha} \right]$  can be finally obtained as shown in (IV-A).

#### APPENDIX C DERIVATION OF (28)

From the expression of  $P'_s$  in (25),  $\mathbb{E}_v [P'_s]$  can be calculated as

$$\begin{aligned} \mathbb{E}_v [P'_s] &= \mathbb{E}_v \left[ \frac{\alpha^{\frac{1}{1+\alpha}}}{b^{\frac{1}{1+\alpha}} v^{\frac{1}{1+\alpha}}} - \frac{1}{v} \right] \Bigg|_{v \geq \frac{b}{\alpha}} \\ &= \underbrace{\int_{\frac{b}{\alpha}}^{\infty} \left( \frac{\alpha}{b} \right)^{\frac{1}{1+\alpha}} x^{-\frac{\alpha}{1+\alpha}} f_v(x) dx}_{\Xi_1} - \underbrace{\int_{\frac{b}{\alpha}}^{\infty} x^{-1} f_v(x) dx}_{\Xi_2}. \quad (57) \end{aligned}$$

Similar to the derivation of (52),  $\Xi_1$  and  $\Xi_2$  can be derived as

$$\begin{aligned} \Xi_1 &= \frac{\alpha_{sd} N_0}{\Gamma(k_1) \eta_1^{k_1}} \sum_{l=0}^{m_{sd}-1} v \frac{(-1)^l (1 - m_{sd})_l (\delta_{sd} N_0)^l}{(l!)^2} \\ &\quad \times \frac{\tilde{k}_1! \alpha^{k_1}}{\tilde{\beta}_{sd}^{k_1+1} b^{k_1}} \frac{1}{\left( \frac{\alpha}{1+\alpha} + k_1 \right)} \\ &\quad \times {}_2F_1 \left( \tilde{k}_1 + 1, \frac{\alpha}{1+\alpha} + k_1; \frac{\alpha}{1+\alpha} + k_1 + 1; -\frac{\alpha}{b \tilde{\beta}_{sd} \eta_1} \right) \quad (58) \end{aligned}$$

and

$$\begin{aligned} \Xi_2 &= \frac{\alpha_{sd} N_0}{\Gamma(k_1) \eta_1^{k_1}} \sum_{l=0}^{m_{sd}-1} \frac{(-1)^l (1 - m_{sd})_l (\delta_{sd} N_0)^l}{(l!)^2} \\ &\quad \times \frac{\tilde{k}_1! \alpha^{k_1}}{\tilde{\beta}_{sd}^{k_1+1} b^{k_1}} \frac{1}{(1 + k_1)} \\ &\quad \times {}_2F_1 \left( \tilde{k}_1 + 1, k_1 + 1; k_1 + 2; -\frac{\alpha}{b \tilde{\beta}_{sd} \eta_1} \right). \quad (59) \end{aligned}$$

By substituting (58) and (59) into (57), and carrying out some mathematical manipulation, we can obtain a closed-form expression for  $\mathbb{E}_v [P'_s]$  as shown in (IV-A).

#### REFERENCES

- [1] V. Joroughi, M. Á. Vázquez, and A. Pérez-Neira, "Generalized multicast multibeam precoding for satellite communications," *IEEE Trans. Wireless Commun.*, vol. 16, no. 2, pp. 952–966, Feb. 2017.
- [2] S. Kandeepan, L. De Nardis, M.-G. Di Benedetto, A. Guidotti, and G. E. Corazza, "Cognitive satellite terrestrial radios," in *Proc. IEEE GLOBECOM*, Miami, FL, USA, Dec. 2010, pp. 1–6.
- [3] Y. Ruan, Y. Li, C.-X. Wang, R. Zhang, and H. Zhang, "Performance evaluation for underlay cognitive satellite-terrestrial cooperative networks," *Sci. China Inf. Sci.*, vol. 61, no. 10, Oct. 2018, Art. no. 102306.
- [4] O. Y. Kolawole, S. Vuppala, M. Sellathurai, and T. Ratnarajah, "On the performance of cognitive satellite-terrestrial networks," *IEEE Trans. Cogn. Commun. Netw.*, vol. 3, no. 4, pp. 668–683, Dec. 2017.
- [5] M. Jia, X. Gu, Q. Guo, W. Xiang, and N. Zhang, "Broadband hybrid satellite-terrestrial communication systems based on cognitive radio toward 5G," *IEEE Wireless Commun.*, vol. 23, no. 6, pp. 96–106, Dec. 2016.
- [6] S. K. Sharma, S. Chatzinotas, and B. Ottersten, "Satellite cognitive communications: Interference modeling and techniques selection," in *Proc. IEEE 6th ASMS/SPSC*, Baiona, Spain, Sep. 2012, pp. 111–118.
- [7] V. Icolari, A. Guidotti, D. Tarchi, and A. Vanelli-Coralli, "An interference estimation technique for satellite cognitive radio systems," in *Proc. IEEE ICC*, London, U.K., Jun. 2015, pp. 892–897.
- [8] K. An, M. Lin, W.-P. Zhu, Y. Huang, and G. Zheng, "Outage performance of cognitive hybrid satellite-terrestrial networks with interference constraint," *IEEE Trans. Veh. Technol.*, vol. 65, no. 11, pp. 9397–9404, Nov. 2016.
- [9] K. An, M. Lin, T. Liang, J. Ouyang, and W.-P. Zhu, "On the ergodic capacity of multiple antenna cognitive satellite terrestrial networks," in *Proc. IEEE ICC*, Kuala Lumpur, Malaysia, May 2016, pp. 1–5.
- [10] S. Maleki, S. Chatzinotas, J. Krause, K. Liolis, and B. Ottersten, "Cognitive zone for broadband satellite communications in 17.3–17.7 GHz band," *IEEE Wireless Commun. Lett.*, vol. 4, no. 3, pp. 305–308, Jun. 2015.
- [11] Z. Li, F. Xiao, S. Wang, T. Pei, and J. Li, "Achievable rate maximization for cognitive hybrid satellite-terrestrial networks with AF-relays," *IEEE J. Sel. Areas Commun.*, vol. 36, no. 2, pp. 304–313, Feb. 2018.
- [12] E. Lagunas, S. K. Sharma, S. Maleki, S. Chatzinotas, and B. Ottersten, "Resource allocation for cognitive satellite communications with incumbent terrestrial networks," *IEEE Trans. Cognit. Commun. Netw.*, vol. 1, no. 3, pp. 305–317, Sep. 2015.
- [13] J. Du, C. Jiang, H. Zhang, X. Wang, Y. Ren, and M. Debbah, "Secure satellite-terrestrial transmission over incumbent terrestrial networks via cooperative beamforming," *IEEE J. Sel. Areas Commun.*, vol. 36, no. 7, pp. 1367–1382, Jul. 2018.
- [14] M. Lin, Z. Lin, W.-P. Zhu, and J.-B. Wang, "Joint beamforming for secure communication in cognitive satellite terrestrial networks," *IEEE J. Sel. Areas Commun.*, vol. 36, no. 5, pp. 1017–1029, May 2018.
- [15] C. Niephaus, M. Kretschmer, and G. Ghinea, "QoS provisioning in converged satellite and terrestrial networks: A survey of the state-of-the-art," *IEEE Commun. Surveys Tuts.*, vol. 18, no. 4, pp. 2415–2441, 4th Quart., 2016.
- [16] Z. Ji, Y. Wang, W. Feng, and J. Lu, "Delay-aware power and bandwidth allocation for multiuser satellite downlinks," *IEEE Commun. Lett.*, vol. 18, no. 11, pp. 1951–1954, Nov. 2014.
- [17] S. Vassaki, A. D. Panagopoulos, and P. Constantinou, "Effective capacity and optimal power allocation for mobile satellite systems and services," *IEEE Commun. Lett.*, vol. 16, no. 1, pp. 60–63, Jan. 2012.
- [18] D. Zhou, M. Sheng, X. Wang, C. Xu, R. Liu, and J. Li, "Mission aware contact plan design in resource-limited small satellite networks," *IEEE Trans. Commun.*, vol. 65, no. 6, pp. 2451–2466, Mar. 2017.
- [19] Y. Ruan, Y. Li, C.-X. Wang, and R. Zhang, "Energy efficient adaptive transmissions in integrated satellite-terrestrial networks with SER constraints," *IEEE Trans. Wireless Commun.*, vol. 17, no. 1, pp. 210–222, Jan. 2018.
- [20] F. Alagoz and G. Gur, "Energy efficiency and satellite networking: A holistic overview," *Proc. IEEE*, vol. 99, no. 11, pp. 1954–1979, Nov. 2011.
- [21] B. Evans, O. Onireti, T. Spathopoulos, and M. A. Imran, "The role of satellites in 5G," in *Proc. EUSIPCO*, Nice, France, Sep. 2015, pp. 2756–2760.
- [22] F. Zhou, N. C. Beaulieu, Z. Li, J. Si, and P. Qi, "Energy-efficient optimal power allocation for fading cognitive radio channels: Ergodic capacity, outage capacity, and minimum-rate capacity," *IEEE Trans. Wireless Commun.*, vol. 15, no. 4, pp. 2741–2755, Apr. 2016.
- [23] B. Liu, F. Zhou, G. Lu, and R. Q. Hu, "Energy efficient and robust beamforming for MISO cognitive small cell networks," *IEEE Internet Things J.*, vol. 5, no. 6, pp. 5002–5014, Dec. 2018.
- [24] S. Shi, G. Li, K. An, B. Gao, and G. Zheng, "Energy-efficient optimal power allocation in integrated wireless sensor and cognitive satellite terrestrial networks," *Sensors*, vol. 17, no. 9, p. 2025, 2017.
- [25] L. Liu, "Energy-efficient power allocation for delay-sensitive traffic over wireless systems," in *Proc. IEEE ICC*, Ottawa, ON, Canada, Jun. 2012, pp. 5901–5905.
- [26] M. Sinaie, A. Zappone, E. A. Jorswieck, and P. Azmi, "A novel power consumption model for effective energy efficiency in wireless networks," *IEEE Wireless Commun. Lett.*, vol. 5, no. 2, pp. 152–155, Apr. 2016.
- [27] B. Li, Z. Fei, Z. Chu, F. Hou, K. K. Wong, and P. Xiao, "Robust chance-constrained secure transmission for cognitive satellite-terrestrial networks," *IEEE Trans. Veh. Technol.*, vol. 67, no. 5, pp. 4208–4219, May 2018.
- [28] S. Maleki *et al.*, "Cognitive spectrum utilization in Ka band multi-beam Satellite communications," *IEEE Commun. Mag.*, vol. 53, no. 3, pp. 24–29, Mar. 2015.
- [29] A. Abdi *et al.* "A new simple model for land mobile Satellite channels: First and second order statistics," *IEEE Trans. Wireless Commun.*, vol. 2, no. 3, pp. 519–528, May 2003.

- [30] Y. Ruan, Y. Li, C.-X. Wang, R. Zhang, and H. Zhang, "Outage performance of integrated satellite-terrestrial networks with hybrid CCI," *IEEE Commun. Lett.*, vol. 21, no. 7, pp. 1545–1548, Jul. 2017.
- [31] I. S. Gradshteyn and I. M. Ryzhik, *Table of Integrals, Series, and Products*, 6th ed. New York, NY, USA: Academic, 2000.
- [32] D. Wu and R. Negi, "Effective capacity: A wireless link model for support of quality of service," *IEEE Trans. Wireless Commun.*, vol. 2, no. 4, pp. 630–643, Jul. 2003.
- [33] P. Patcharamaneepakorn *et al.*, "Spectral, energy, and economic efficiency of 5G multicell massive MIMO systems with generalized spatial modulation," *IEEE Trans. Veh. Technol.*, vol. 65, no. 12, pp. 9715–9731, Dec. 2016.
- [34] R. Zhang, Y. Li, C.-X. Wang, Y. Ruan, Y. Fu, and H. Zhang, "Energy-spectral efficiency trade-off in underlaying mobile D2D communications: An economic efficiency perspective," *IEEE Trans. Wireless Commun.*, vol. 17, no. 7, pp. 4288–4301, Jul. 2018.
- [35] Y. Ruan, Y. Li, C.-X. Wang, R. Zhang, and H. Zhang, "Effective capacity analysis for underlay cognitive satellite-terrestrial networks," in *Proc. IEEE ICC*, Paris, France, May 2017, pp. 1–6.
- [36] F. Haider, C.-X. Wang, X. Hong, H. Haas, D. Yuan, and E. Hepsaydir, "Spectral-energy efficiency tradeoff in cognitive radio networks with peak interference power constraints," in *Proc. IEEE ICCT*, Jinan, China, Sep. 2011, pp. 368–372.
- [37] N. I. Miridakis, D. D. Vergados, and A. Michalakis, "Dual-hop communication over a satellite relay and shadowed Rician channels," *IEEE Trans. Veh. Technol.*, vol. 64, no. 9, pp. 4031–4040, Sep. 2015.
- [38] A. Charnes and W. W. Cooper, "Programming with linear fractional functionals," *Naval Res. Logistics Quart.*, vol. 9, nos. 3–4, pp. 181–186, Sep./Oct. 1962.
- [39] S. Schaible, "Parameter-free convex equivalent and dual programs of fractional programming problems," *Oper. Res.*, vol. 18, no. 5, pp. 187–196, 1974.
- [40] A. Zappone and E. Jorswieck, "Energy efficiency in wireless networks via fractional programming theory," *Found. Trends Commun. Inf. Theory*, vol. 11, nos. 3–4, pp. 185–396, 2015.
- [41] S. Boyd and L. Vandenberghe, *Convex Optimization*. Cambridge, U.K.: Cambridge Univ. Press, 2004.
- [42] A. Ghasemi and E. S. Sousa, "Fundamental limits of spectrum-sharing in fading environments," *IEEE Trans. Wireless Commun.*, vol. 6, no. 2, pp. 649–658, Feb. 2007.



**Yuhuan Ruan** received the B.S. and Ph.D. degrees in telecommunications engineering from Xidian University, Xi'an, China, in 2013 and 2018, respectively. She was a Visiting Ph.D. Student under the supervision of Prof. C.-X. Wang in Heriot-Watt University, Edinburgh, U.K., from 2016 to 2017. In 2018, she joined the School of Telecommunications Engineering, Xidian University, where she is currently a Lecturer. Her current research interests are in the fields of satellite-terrestrial networks, cooperative communications, cognitive radio techniques, and energy efficient wireless networks.



**Yongzhao Li** (M'04–SM'17) received the B.S., M.S., and Ph.D. degrees in electronic engineering from Xidian University, Xi'an, China, in 1996, 2001, and 2005, respectively. Since 1996, he joined Xidian University, where he is currently a Full Professor with the State Key Laboratory of Integrated Services Networks. As a Research Professor, he was with the University of Delaware, Delaware, USA, from 2007 to 2008, and the University of Bristol, Bristol, U.K., in 2011, respectively. He currently serves as the Vice Dean of the School of Telecommunications Engineering, Xidian University. He has published more than 50 journal papers and 20 conference papers. His research interests include wideband wireless communications, signal processing for communications, and spatial communications networks. In 2008, he received the Best Paper Award of the IEEE ChinaCOM'08 International Conference. Due to his excellent contributions in education and research, in 2012, he was awarded by the Program for New Century Excellent Talents in University, Ministry of Education, China.



**Cheng-Xiang Wang** (S'01–M'05–SM'08–F'17) received the B.Sc. and M.Eng. degrees in communication and information systems from Shandong University, China, in 1997 and 2000, respectively, and the Ph.D. degree in wireless communications from Aalborg University, Denmark, in 2004.

He was a Research Assistant with the Hamburg University of Technology, Hamburg, Germany, from 2000 to 2001, a Research Fellow with the University of Agder, Grimstad, Norway, from 2001 to 2005, and a Visiting Researcher with Siemens AG-Mobile Phones, Munich, Germany, in 2004. He has been with Heriot-Watt University, Edinburgh, U.K., since 2005, where he became a Professor in wireless communications in 2011. In 2018, he joined Southeast University and Purple Mountain Laboratories, Nanjing, China, as a Professor. He has coauthored three books, one book chapter, more than 350 journals and conference papers, including over 120 papers published in various IEEE journals/magazines and 23 ESI Highly Cited Papers. He has also delivered 17 invited Keynote Speeches/Talks and 7 tutorials in international conferences. His current research interests include wireless channel measurements/modeling, B5G wireless communication networks, and applying artificial intelligence to wireless communication networks.

Dr. Wang is a fellow of the IET, an IEEE Communications Society Distinguished Lecturer for 2019 and 2020, and a Highly Cited Researcher recognized by Clarivate Analytics in 2017 and 2018. He was a recipient of ten Best Paper Awards from the IEEE GLOBECOM 2010, IEEE ICCT 2011, ITST 2012, IEEE VTC 2013-Spring, IWCMC 2015, IWCMC 2016, IEEE/CIC ICC 2016, WPMC 2016, and WOCC 2019. He has served as a technical program committee (TPC) member, the TPC chair, and the general chair for more than 80 international conferences. He is currently an Executive Editorial Committee (EEC) Member of the IEEE TRANSACTIONS ON WIRELESS COMMUNICATIONS. He has served as an Editor for nine international journals, including the IEEE TRANSACTIONS ON WIRELESS COMMUNICATIONS from 2007 to 2009, the IEEE TRANSACTIONS ON VEHICULAR TECHNOLOGY from 2011 to 2017, and the IEEE TRANSACTIONS ON COMMUNICATIONS from 2015 to 2017. He was a Guest Editor of the IEEE JOURNAL ON SELECTED AREAS IN COMMUNICATIONS, Special Issue on Vehicular Communications and Networks (Lead Guest Editor), Special Issue on Spectrum and Energy Efficient Design of Wireless Communication Networks, and Special Issue on Airborne Communication Networks. He was also a Guest Editor of the IEEE TRANSACTIONS ON BIG DATA, Special Issue on Wireless Big Data, and the IEEE TRANSACTIONS ON COGNITIVE COMMUNICATIONS AND NETWORKING, Special Issue on Intelligent Resource Management for 5G and Beyond.



**Rui Zhang** received the B.S., M.S., and Ph.D. degrees in telecommunications engineering from Xidian University, Xi'an, China, in 2012, 2015, and 2018, respectively. He was a Visiting Student under the supervision of Prof. C.-X. Wang in Heriot-Watt University, Edinburgh, U.K., from 2016 to 2017. His current research interests focus on device-to-device (D2D) communications, vehicle-to-vehicle (V2V) communications, radio resource allocation techniques, and energy efficient wireless networks.



**Hailin Zhang** (M'98) received the B.S. and M.S. degrees from Northwestern Polytechnic University, Xi'an, China, in 1985 and 1988, respectively, and the Ph.D. degree from Xidian University, Xi'an, in 1991. Since 1991, he has been with Xidian University, where he is currently a Senior Professor and a Ph.D. Adviser with the School of Telecommunications Engineering. He is currently the Director of the Key Laboratory in Wireless Communications Sponsored by China Ministry of Information Technology, a Key Member of the State Key Laboratory of Integrated Services Networks, one of the State Government Specially Compensated Scientists and Engineers, a Field Leader in telecommunications and information systems with Xidian University, and the Associate Director of National 111 Project. He has recently published 78 papers in telecommunications journals and proceedings. His current research interests include key transmission technologies and standards on broadband wireless communications for 4G, 5G, and next generation broadband wireless access systems.